Electronic Supplementary Material (ESI) for Journal of Materials Chemistry

Supplementary Information

Porous carbon-modiifed MnO disks prepared by a microwave-polyol process and their superior lithium-ion storage properties

Yongming Sun, Xianluo Hu,* Wei Luo, and Yunhui Huang*

E-mail: huxl@mail.hust.edu.cn (or xlhu07@gmail.com); huangyh@mail.hust.edu.cn

State Key Laboratory of Material Processing and Die & Mould Technology, College of Materials Science and Engineering, Huazhong University of Science and Technology, Wuhan 430074, P. R. China

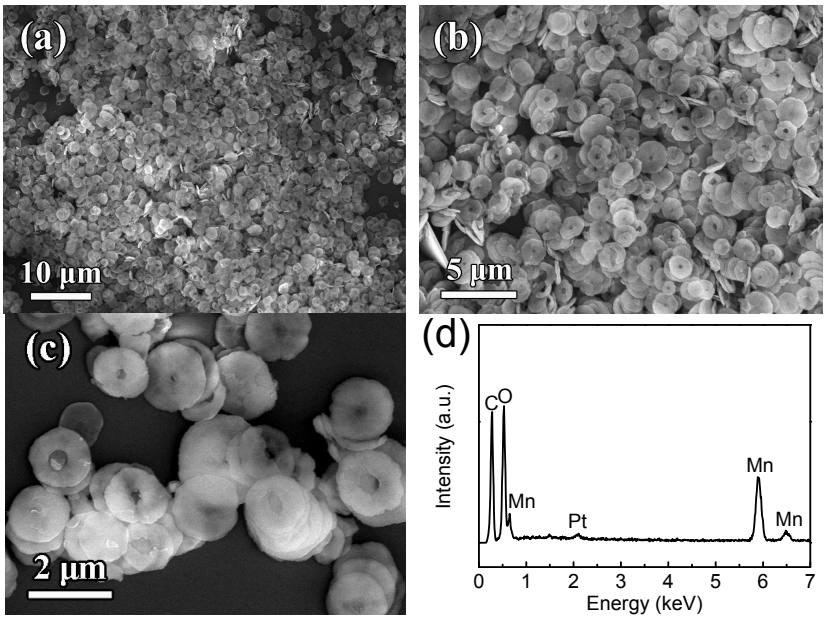

Fig. S1 (a-c) FESEM images, and (d) a typical EDX pattern for the Mn-complex precursor obtained by a microwave-polyol process at 195 ºC for 10 min. The signal of Pt is generated from the surface coating of Pt by sputtering to minimize charging effects under SEM imaging conditions.

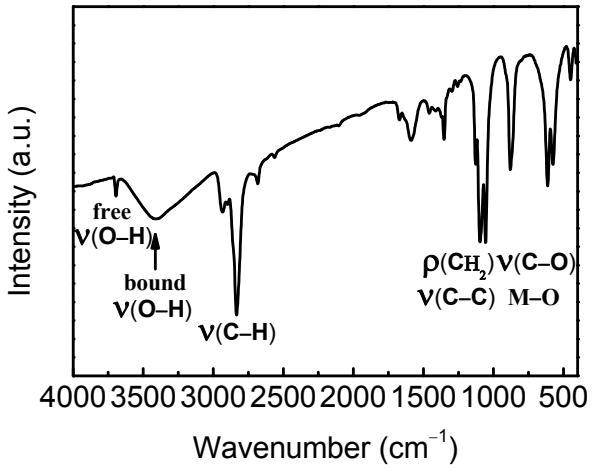

Fig. S2 A typical FT-IR spectrum for the Mn-based precursor.

The presence of glycolated species in the Mn-based precursor was confirmed, compared with the FT-IR spectrum of liquid ethylene glycol.[1] The strong absorption bands in the range of 2500–3000 cm^{-1} were observed, characteristic of the C–H stretching mode. The broad band at 3413 cm^{-1} and the sharp band at 3600 cm^{-1} arise from the hydrogen-bound hydroxyl groups and structurally isolated hydroxyls, respectively. The band at around 1620 cm^{-1} is attributed to the δH_2O-bending signal.[2] The peaks below 2000 cm^{-1} (except 1620 cm^{-1}) correspond to $\rho(CH_2)$, $\gamma(CH_2)$, υ(C–O), υ(C–C) and metal-O bands.[2, 3] There is no absorption at around 1700 cm^{-1}, indicating the absence of carboxyl groups, and thus there are no acetate groups in the precursor.[2] The FT-IR results reveal that the ethylene glycolate anions in the precursor and there remains no PVP in the precursor. Thus, the intermediate is manganese glycolate. There is no N peak in the EDX pattern of the precursor and the carbon in the C-MnO product may originate from the decomposition of the ethylene glycolate anions during the heat treatment of the precursor in a 5% H_2/Ar atmosphere.

1) N. Chakroune, G. Viau, S. Ammar, N. Jouini, P. Gredin, M. J. Vaulay and F. Fiévet, *New J. Chem.*, 2005, **29**, 355.
2) D. Larcher, G. Sudant, R. Patrice and J. M. Tarascon, *Chem. Mater.*, 2003, **15**, 3543.
3) D. Groeneveld and W. L. Groeneveld, *Inorg. Chim. Acta*, 1973, **7**, 81.

.

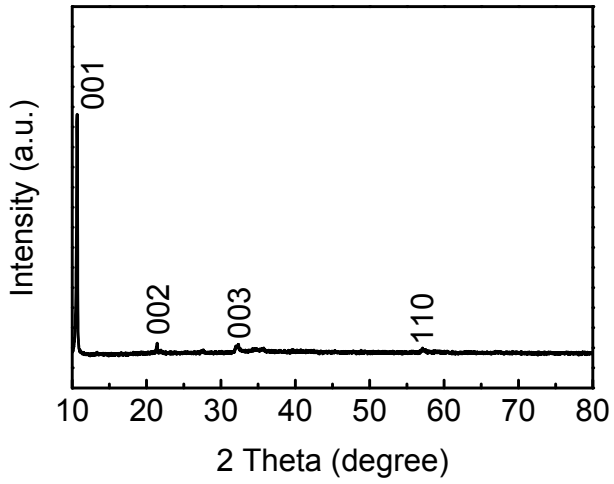

Fig. S3 A typical XRD pattern for the Mn-based precursor.

The Mn-based precursor presents a layered structure derived from the brucite structure [space group: $P\bar{3}m1$ (164)]. The main peaks in the XRD pattern can be indexed to (001), (002), (003), and (110) planes in the hexagonal system, characteristic of a brucite structure. The narrow (00*l*) peaks reveal a large correlation length along the [001] direction. The interlayer spacing of the brucite structure is calculated to be about 8.3 Å, corresponding to the lattice constant of *c*. Obviously, it is much larger than that of the general inorganic materials with a brucite structure, such as $Mg(OH)_2$ (JCPDS No. 44–1482; c = 4.8 Å), $Co(OH)_2$ (JCPDS No. 30–0443; c = 4.7 Å), or $Ca(OH)_2$ (JCPDS No. 44–1481; c = 4.9 Å). As the structure of the Mn-based precursor can be described as the stacked metal-oxygen sheets separated by bonded alcoholate anions, these large alcoholate anions in the interlayers elongate the distance between the metal-oxygen sheets. In the brucite structure, the lattice constant of a (or b) corresponds to the smallest metal–metal distance within the triangular array of the (ab) layer. In the obtained Mn-based precursor, the Mn–Mn distance, deduced from the (110) peak in the XRD pattern, is about 3.2 Å, much close to the general inorganic brucite-structured materials, such as $Mg(OH)_2$ (JCPDS No. 44–1482; a = 3.1 Å), $Co(OH)_2$ (JCPDS No. 30–0443; a = 3.2 Å) and $Ca(OH)_2$ (JCPDS No. 44–1481; a = 3.6 Å). Moreover, it is confirmed that the metal ions are located on the octahedral sites in their crystal structures. Thus, it can be concluded that the extract structure of the (*ab*) layer is very similar to the inorganic brucite-structured materials and no alcoholate anions exist in the (*ab*) layer. Combined with the large interlayer distance along the c axes in the structure, the lattice constants can be finally identified as $a = b$ = 3.2 Å, c = 8.3 Å, $\alpha = \beta = 90^\circ$, $\gamma = 120^\circ$.

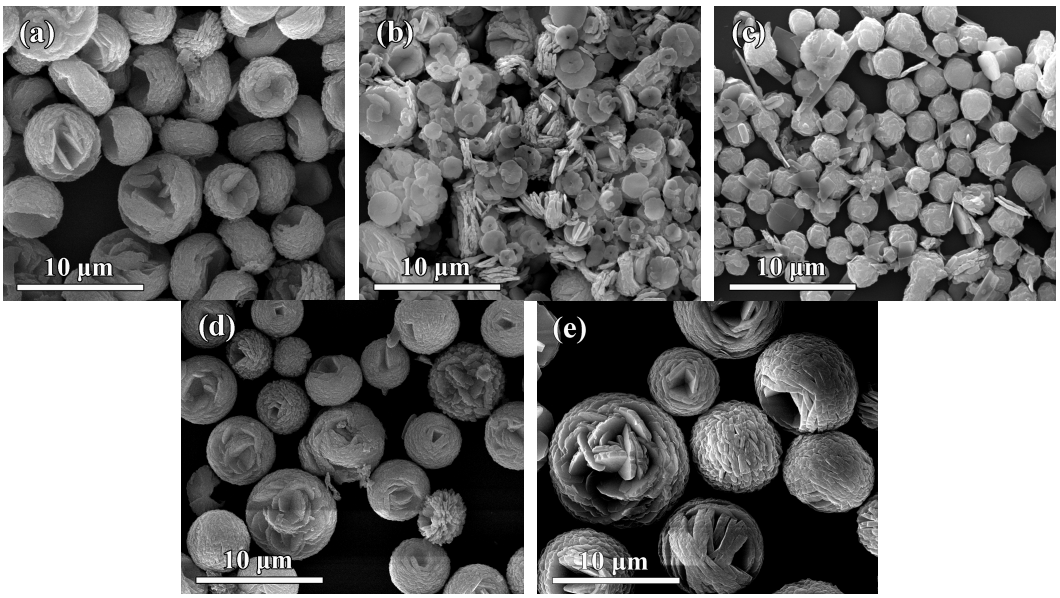

Fig. S4 FESEM images of the products prepared under different conditions: (a) 2 mmol of $Mn(OAc)_2 \cdot 4H_2O$, (b) 2 mmol of $Mn(OAc)_2 \cdot 4H_2O$ and 0.1 g PVP, (c) 2 mmol of $Mn(OAc)_2 \cdot 4H_2O$ and 0.8 g of PVP, (d) 0.8 mmol of $Mn(OAc)_2 \cdot 4H_2O$ and 0.4 g of PVP, (e) 4 mmol of $Mn(OAc)_2 \cdot 4H_2O$ and 0.4 g of PVP in 50 ml of ethylene glycol.

It is found that both PVP and the reactant concentration play a crucial role in the formation of uniform Mn-alkoxide disks. PVP serves as a soft template that directs the formation of disks and avoids the aggregation of the resulting disks.

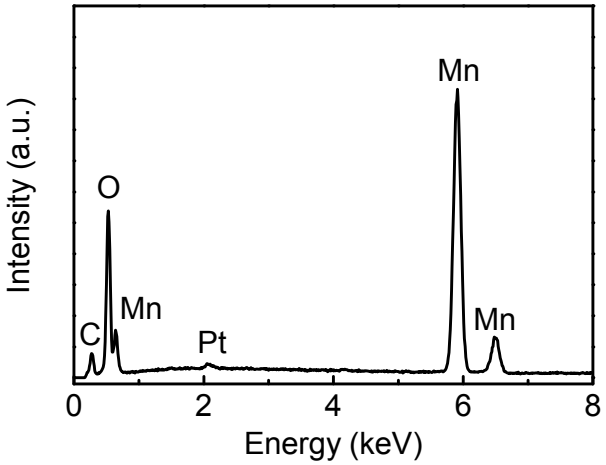

Fig. S5 A typical EDX spectrum of the C-MnO disks.

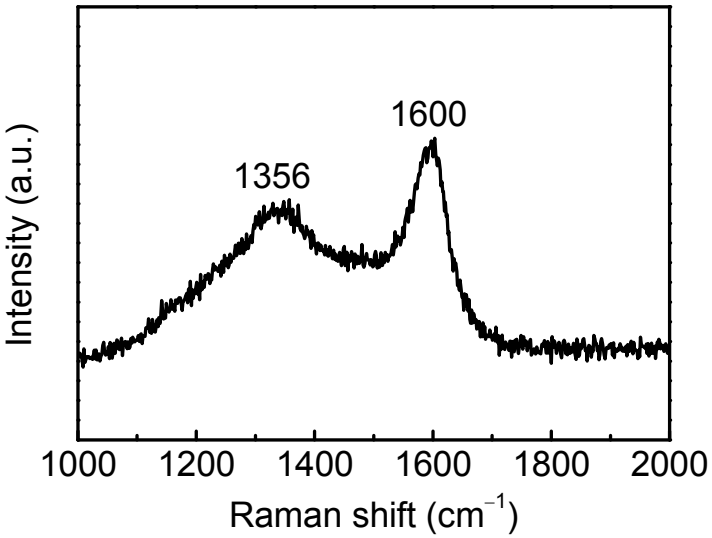

Fig. S6 Raman spectrum of the as-formed porous C-MnO disks. The peaks at around 1356 and 1600 cm^{-1} are attributed to the characteristic D-band and G-band of carbon, respectively.

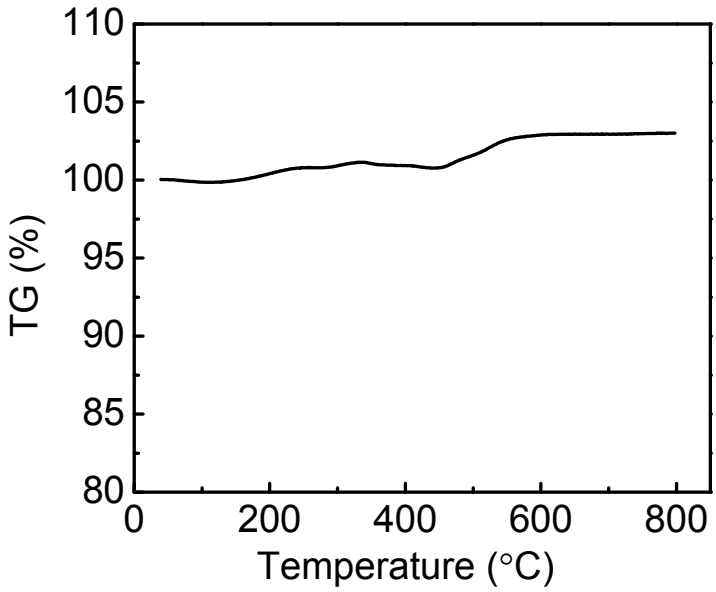

Fig. S7 TG result for the carbon modified MnO disks measured at a heating rate of 10 ºC min^{-1} in a flowing air. The weight change between 100 and 700 °C is due to the oxidation of the MnO and the combustion of carbon. The total weight increase of the sample between 100 and 700 °C is 3.1 wt %. The final product after the TG measurement is Mn_2O_3 (evidenced by the XRD result). Thus, the carbon content in the final product is evaluated to be about 7.3 wt %.

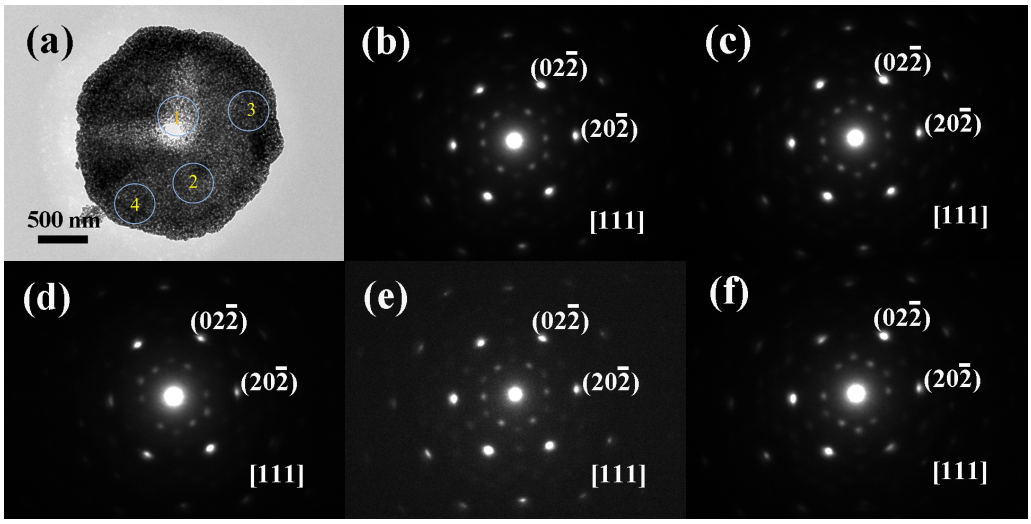

Fig. S8 (a) TEM image of a single disk. The SAED patterns were recorded from the whole disk, and the different domains: (b) whole disk, (c) cycle 1, (d) cycle 2, (e) cycle 3, and (f) cycle 4.

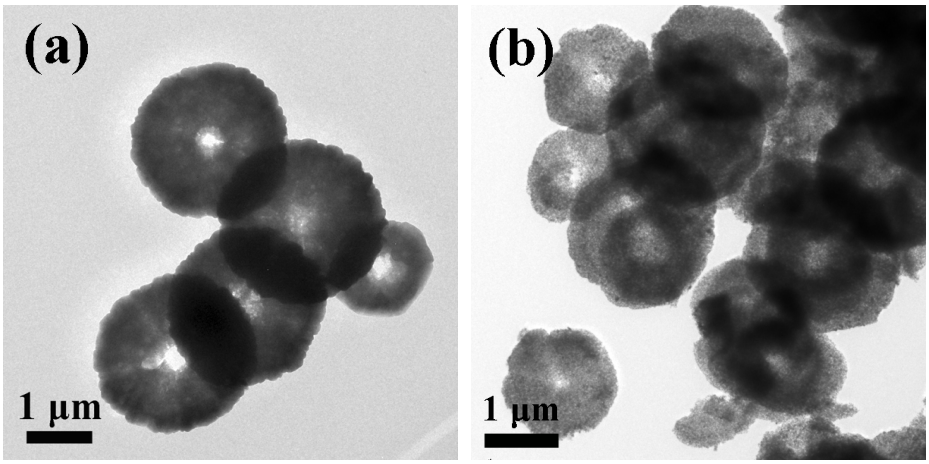

Fig. S9 TEM images of (a) the Mn-based precursor and (b) the carbon-modified MnO disks.

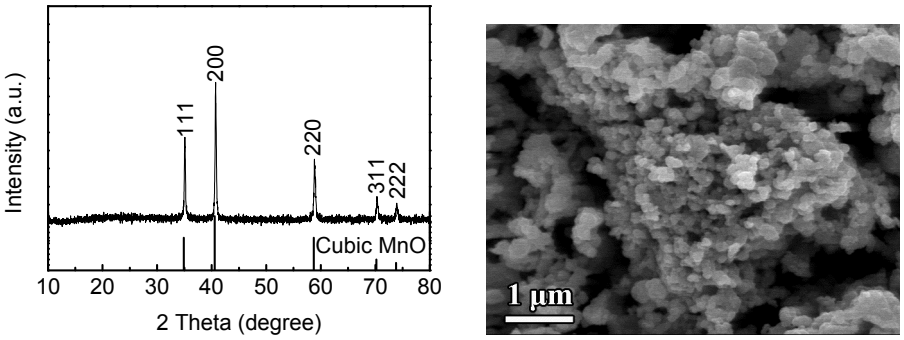

Fig. S10 XRD pattern (left) and SEM image (right) of carbon-free MnO particles prepared by heating $Mn(OAc)_2 \cdot 4H_2O$ in 5% H_2/Ar at 700 °C for 5 h.

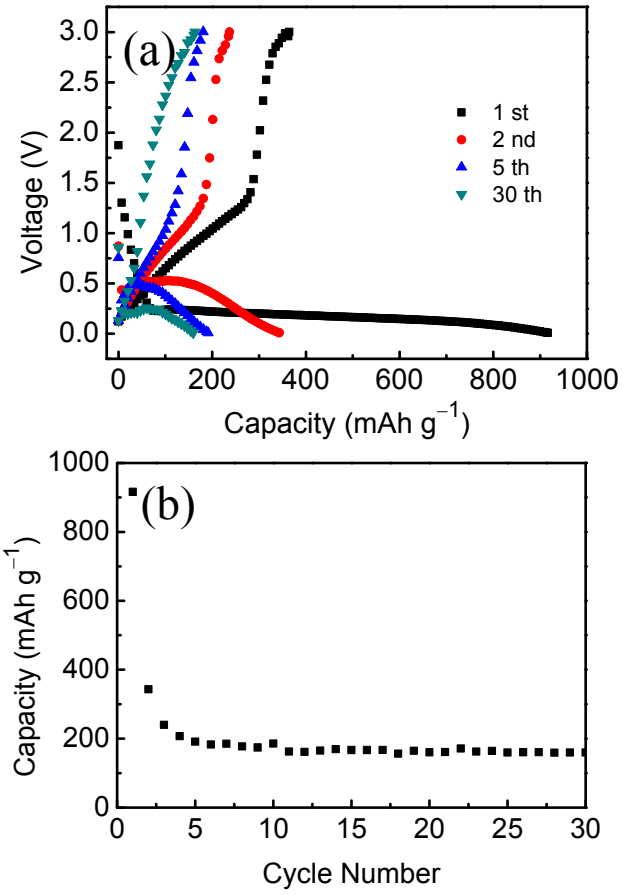

Fig. S11 (a) Discharge and charge curves and (b) cycling performance of the electrode made of carbon-free MnO particles at 200 mA g^{-1}.